

Green Chemistry

Accepted Manuscript



This article can be cited before page numbers have been issued, to do this please use: N. S. Date, A. Hengne, K. Huang, R. C. Chikate and C. V. Rode, *Green Chem.*, 2018, DOI: 10.1039/C8GC00284C.



This is an Accepted Manuscript, which has been through the Royal Society of Chemistry peer review process and has been accepted for publication.

Accepted Manuscripts are published online shortly after acceptance, before technical editing, formatting and proof reading. Using this free service, authors can make their results available to the community, in citable form, before we publish the edited article. We will replace this Accepted Manuscript with the edited and formatted Advance Article as soon as it is available.

You can find more information about Accepted Manuscripts in the [author guidelines](#).

Please note that technical editing may introduce minor changes to the text and/or graphics, which may alter content. The journal's standard [Terms & Conditions](#) and the ethical guidelines, outlined in our [author and reviewer resource centre](#), still apply. In no event shall the Royal Society of Chemistry be held responsible for any errors or omissions in this Accepted Manuscript or any consequences arising from the use of any information it contains.



Journal Name

ARTICLE

Single Pot Selective Hydrogenation of Furfural to 2-Methylfuran Over Carbon Supported Iridium Catalysts

Nandan S. Date^{a,b}, Amol M. Hengne^c, K-W Huang^c, Rajeev C. Chikate^{b*}, Chandrashekhar V. Rode^{a*}

Received 00th January 20xx,
Accepted 00th January 20xx

DOI: 10.1039/x0xx00000x

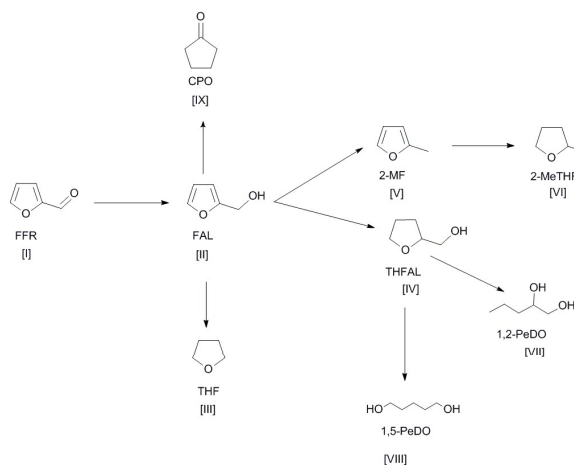
www.rsc.org/

Various iridium supported carbon catalysts were prepared and screened for direct hydrogenation of furfural (FFR) to 2-methyl furan (2-MF). Amongst these, 5% Ir/C showed excellent results with complete FFR conversion and highest selectivity of 95% to 2-MF at very low H₂ pressure of 100 psig. Metallic (Ir⁰) and oxide (IrO₂) phases of Ir catalyzed first step hydrogenation involving FFR to FAL and subsequent hydrogenation to 2-MF, respectively. This was confirmed by XPS analysis and some controlled experiments. At low temperature of 140 °C, almost equal selectivities of FAL (42%) and 2-MF (43%) were observed, while higher temperature (220 °C) favored selective hydrodeoxygenation. At optimized temperature, 2-MF formed selectively while higher pressure and higher catalyst loading favored ring hydrogenation of furfural rather than side chain hydrogenation. With combination of several control experimental results and detailed catalyst characterization, a plausible reaction pathway has been proposed for selective formation of 2-MF. The selectivity to various other products in FFR hydrogenation can be manipulated by tailoring the reaction conditions over the same catalyst.

Introduction

Transformation of lignocellulosic biomass into fine chemicals and various workable merchandises is gaining more importance in pursuit of alternatives for petroleum based fuels and chemicals.¹⁻³ Among the variety of bio-derived feedstock options, abundantly available lignocellulosic material at a lower cost can be easily converted into a variety of platform molecules. Efficient transformation of these platform molecules with maximum selectivity to a useful product in a multiproduct reaction becomes a very interesting challenge in terms of catalyst design and process competitiveness.^{2,4} According to DOE report of 2004, furfural is considered as a key platform moiety in the development of lignocellulose based bio-refinery. It is mainly derived by acid dehydration of arabinose and xylose which are obtained from unused agriculture waste such as corncobs, wood residue etc.^{5,6} Furfural is a major component of biomass derived bio oil and its current global production is almost 50,00,000 tpa. However limited intensification techniques and tedious isolation problems are the main drawbacks in efficient conversion of FFR into C5 chemicals.⁶⁻⁷ Main hydrogenation products of furfural are obtained by the reduction of C=O bond and

subsequent hydrogenation of aromatic ring to produce furfuryl alcohol, tetrahydrofurfuryl alcohol, pentanediols, 2-methyl furan, methyl tetrahydrofuran, cyclopentanone etc. (Scheme 1)^{7,8} which constitute the key fuel additives and starting monomers.



Scheme 1: General furfural hydrogenation scheme

For example, 2-MF is a fine chemical arising from furfural via selective hydrogenation of C=O bond. Being considered as a green solvent, it has vast uses in bio-refinery as well as in chemical industries. Its water miscible nature and solubility in many organic solvents makes it useful for the formation of building blocks in the pharmaceutical industry. 2-MF is also

^a N. S. Date, Dr. C. V. Rode* CEPD, CSIR-NCL, Dr Homi Bhabha Road, Pashan, Pune-411008.

^b N.S. Date, Prof. R. C. Chikate* Post-graduate & research centre, Department of Chemistry, M. E. S. S. Abasaheb Garware college of Arts and Science, Karve road, Pune-411004.

^c A. M. Hengne, K-W Huang. KAUST Catalysis Center and Division of Physical Sciences and Engineering, King Abdullah University of Science and Technology, Thuwal, 23955-6900, Kingdom of Saudi Arabia.

* Corresponding author: cv.rode@ncl.res.in

ARTICLE

Journal Name

used as a starting material in the production of toluene on a commercial scale. It shows good combustion performance and high energy density similar to 2-MeTHF, also RON of 2-MF is greater than that of gasoline, which can be a good alternative to gasoline.⁹⁻¹⁴ Efficient and selective conversion of furfural to other by-products mainly depends on appropriate catalyst design and substrate-metal/support interactions or adsorption of substrate.

2-MF production is possible by selective hydrodeoxygenation of FFR without affecting the furanic "O" as well the ring double bonds.⁷ In the last decade, various types of catalyst systems were developed for the synthesis of 2-MF from furfural either via direct hydrogenation using H₂ or via catalytic transfer hydrogenation using IPA. Catalysts containing chromium were reported to be very efficient for selective conversion of FFR to 2-MF but have a problem of their inherent toxicity.¹⁵ Recently, Ni-Cu or Fe-Cu, Fe-Ni alloy catalysts have been reported for synthesis of 2-MF with high yield but they possess serious deactivation problems.¹⁶⁻¹⁹ Sitthisa et al. have reported various silica supported nickel and copper catalysts for selective conversion of furfural to 2-methyl furan.²⁰⁻²² Catalyst systems containing Cu, Cr, Zn with varying metal compositions showed excellent performance giving 98% FFR conversion with more than 90% selectivity to 2-MF, with excellent stability and recyclability.^{23,24} Vlachos et al. reported a carbon supported Ru catalyst system where 61% yield of 2-MF was achieved through CTH using IPA.²⁵ The same group recently reported a nano-porous Cu-Al-Co ternary alloy catalyst system where 66% yield of 2-MF was possible at higher temperature of 240 °C.²⁶ In a similar manner, Hermans et al. also reported CTH of FFR to 2-MF over Pd/Fe₂O₃ giving 62% 2-MF yield.²⁷ Various reports are also available on Cu containing bimetallic catalysts in combination with another oxophilic metal showing a comparable selectivity to 2-MF from FAL through HDO process.²⁸⁻³¹ Recently, a new catalyst based on molybdenum is considered to be very active and selective for furfural conversion to 2-MF where 2-MeF selectivity of 60% is reported at low temperature.^{32,33} In recent papers, DFT study were carried over different catalysts.³⁴ In our recent study of furfural hydrogenation over boron doped Pd/C catalysts, 2-MF selectivity achieved was only 35-45%. It was found that the selectivities could be switched to ring hydrogenated and decarbonylation products by controlling the catalyst particle size however, achieving the highest selectivity to only hydrodeoxygenation product like 2-MF was not possible over Pd/C catalyst.³⁵ Hence in the present work, we focused our efforts on developing a catalyst system for furfural hydrogenation to 2-methylfuran with a maximum selectivity up to 95 %. Not only the structure activity correlation was established for our novel Ir based catalyst system by detailed characterization but also the product selectivity could be tuned by varying the different reaction conditions.

Experimental

Materials

Furfural, furfuryl alcohol, tetrahydrofurfuryl alcohol, 2-methylfuran, 2-methyltetrahydrofuran, pentanediols along with Al₂O₃, SiO₂ and TEOS were purchased from Sigma Aldrich, Bangalore, India. IrCl₃.3H₂O was purchased from Johnson Matthey. Sodium hydroxide and sodium borohydride were purchased from Thomas Baker, India. Hydrogen gas was obtained from Vadilal Chemicals Pvt. Ltd. Mumbai, India.

Pre-treatment of carbon

5g charcoal was dispersed in 100 mL of 10 % sulphuric acid solution and stirred for 6h at 65 °C. The solid was filtered and washed successively with DI water till neutrality. This cake was dried at 85 °C for overnight and used for preparation of catalysts.

Catalyst preparation for Ir/C

All the catalysts were prepared by wet impregnation method as per previously reported procedure.³⁵ For the preparation of 1g of 5 % Ir/C catalyst, 91mg of IrCl₃ was first dissolved in 50ml DI water and stirred for 10 min. To this, slurry of 0.95 g activated carbon in water was added slowly with constant stirring and whole mixture was stirred for 2 h. 5M NaOH solution was then added to the above solution till pH was close to 7 and stirring was continued for further 30 minutes. To the above solution, 0.5g NaBH₄ was added in small portions and mixture was stirred for 30 min under inert atmosphere. The catalyst was filtered, washed several times with DI water and kept for drying in oven at 110 °C. Similar procedures was adopted for preparation of 1-6 % Ir/C catalysts. Similar protocol was adopted for the synthesis of 5 % Ir on various supports like Al₂O₃, SiO₂, Mont K10, TiO₂.

Catalyst characterization

The X-ray diffraction measurement was carried out on Shimadzu 6100 using Cu-K α for crystallinity and the phase purity analysis of Ir/C samples. HR-TEM images of catalysts were obtained the particle size and morphology were studied using transmission electron microscope model JEOL 1200 EX. BET surface area and ammonia TPD of all Ir-supported catalysts were obtained using the DFT method on a Quantachrom3 iQ2. XPS analysis was carried out on Thermo Fisher Scientific Instrument. The spectra were excited by low power Al K α X-ray source and analyzer was operated in the constant analyzer energy (CAE) mode. Pyridine FT-IR spectra of the prepared catalysts were recorded on a Perkin Elmer 2000 FTIR spectrometer in the 4000–400 cm⁻¹ wave number range using the KBr pellet technique.

Typical procedure for catalytic hydrogenation of furfural

Catalytic hydrogenation of furfural was performed in a 300 ml stainless steel autoclave equipped with overhead stirrer, a pressure gauge and automatic temperature control apparatus. In a typical experiment, 2.5 g furfural in 95 ml IPA, and catalyst (0.25 g) were loaded into the reactor. It was then sealed and purged with H₂ for 2 times to exclude air. H₂ was charged into

the reactor, when the autoclave temperature reached to desired temperature. The samples were withdrawn from time to time for monitoring the progress of the reaction with GC analysis.

Product analysis

Timely samples were collected and analyzed on Thermo TRACE 700 GC using HP-5 capillary column having dimensions 30 m x 0.32 mm x 0.25 μ m with a flame ionization detector. The following temperature program method was used for GC analysis: 40 $^{\circ}$ C (3 min), 1 $^{\circ}$ C/min, 45 $^{\circ}$ C (1 min), 100 $^{\circ}$ C/min, 60 (0 min), 200 $^{\circ}$ C/min, and 250 (1 min). Performance of 5 % Ir/C catalyst was evaluated in terms of (%) conversion of FFR and (%) product selectivity that are defined below.

$$\% \text{ Conversion} = \frac{\text{Moles of FFR consumed}}{\text{Initial moles of the furfural}} \times 100$$

$$\% \text{ Selectivity} = \frac{\text{Moles of product formed}}{\text{Total moles of all product formed}} \times 100$$

Results and discussion

Main goal of the present work was to achieve maximum selectivity to 2-MF in a single step catalytic hydrodeoxygenation of FFR. This transformation involves firstly, hydrogenation of FFR to FAL with simultaneous hydrodeoxygenation to 2-MF with loss of one water molecule. In our previous work on catalyst screening for FFR hydrogenation, Ir supported on C showed 83 % selectivity to 2-MF with suppression of by-products formation.³⁵ In continuation, detail catalyst characterization for understanding the observed highest selectivity to 2-MF is discussed below.

Catalyst characterization

BET surface area

A series of iridium C supported catalyst were prepared with varying metal loadings from 1% to 6% and their surface area values are presented in Table S1. BET surface area of bare carbon support was 108 m^2/g , with increase in metal loading from 1% to 6%. There was gradual increase in surface area from 117 m^2/g to 215 m^2/g . Linear increase in surface area may be due to agglomeration of iridium nanoparticles on the surface of carbon, surface modification of carbon pore structure during pre-treatment of carbon support and time of reduction with NaBH_4 .³⁶

XRD

X-ray diffraction of 1-6 % Ir/C catalyst with bare carbon support is shown in figure 1. A broad characteristics peak at $2\theta = 24.80^{\circ}$ corresponds to (002) plane, representing the amorphous phase of layered graphitic carbon. A second peak was observed at $2\theta = 44.15^{\circ}$, representing a characteristic plane of (100) of rhombohedral structure of carbon. These planes resemble the planes of turbostratic carbon peak or the presence of graphitic carbon.^{35,37} After impregnation of Ir on carbon support, no any characteristic peaks of iridium species

were observed. This suggests that Ir dispersion on carbon was of an amorphous nature or overlap of the characteristic peaks of iridium with those of carbon. Amorphous nature of catalyst in which formation of small cluster of active sites on the surface results in small particle sizes could be responsible for high activity towards furfural hydrogenation to give 2-MF.³⁸ Further study was done with 5% Ir/C catalyst.

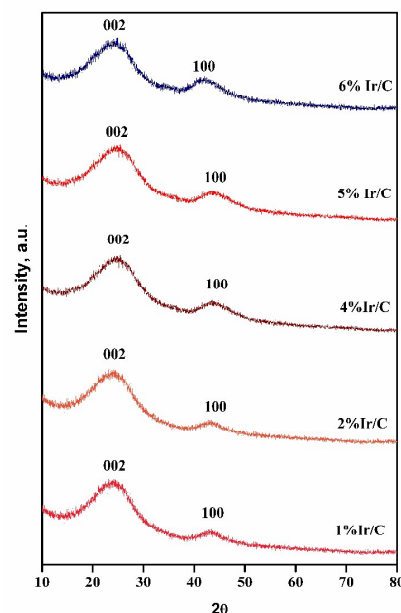


Figure 1: XRD graphs of 1% to 6% Ir/C catalysts

XPS

In order to examine chemical composition as well as electronic states of the metal functions in various catalyst samples, XPS study was carried out and the results are shown in Figure 2.

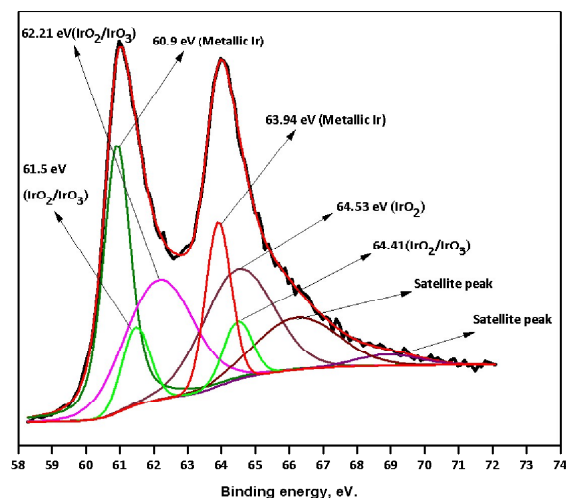


Figure 2A: XPS spectra of Fresh 5% Iridium/ Carbon-Iridium 4f

The binding energy values (B.E.) for all the catalysts were interpreted after applying the charge correction using C1s

ARTICLE

Journal Name

spectra (B.E. 284.6 eV). Figure 2A shows XPS spectra of Ir 4f of 5% Ir/C catalyst, where splitting of Ir 4f peak into $4f_{5/2}$ and $4f_{7/2}$ is due to spin orbit coupling of the 4f orbital (3.1 eV). Additionally, satellite peaks were observed in the $4f_{5/2}$ region of spectrum, which is 4 eV above the region of $4f_{7/2}$, this is mainly due to the structured electron-hole pair excitation. More intense peak as a doublet was observed at BE of 60.98 eV implying that iridium monolayer formed was of rutile type and was confirmed by the presence of metallic Ir peak at BE = 60.86 eV which is analogous to the previous literature.³⁹ After deconvolution, total 9 peaks of the core level Ir 4f spectra were observed among which seven peaks could be ascribed to $4f_{7/2}$ and $4f_{5/2}$ along with two satellite peaks. In $4f_{7/2}$ region, 3 overlapping peaks were obtained at BE = 60.9 eV, 61.5 eV and 62.21 eV which were corresponding to the metallic Ir, IrO_2 and IrO_3 , respectively.^{39,40} Similarly, the $4f_{5/2}$ region showed peaks at BE = 63.94 eV, 64.41 eV and 64.53 eV. Shifting of these peaks at lower binding energy suggests that there was absence of bulk oxide species.^{41,40} The peaks observed at BE = 66.31 eV and 69.21 eV were considered as satellite peaks of iridium.

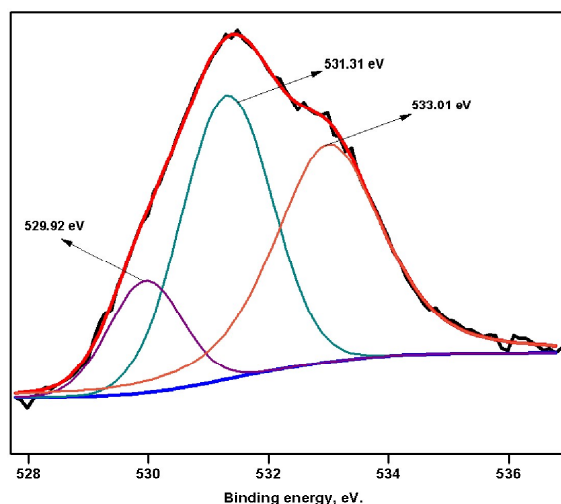


Figure 2B: XPS spectra of Fresh 5% Iridium/ Carbon- Oxygen 1s

Deconvoluted oxygen 1s core level spectra in Figure 2B, shows three distinct peaks of oxygen 1s spectra at B.E. = 529.92 eV, 531.31 eV and 533.01 eV. Both peaks at B.E. = 529.92 eV and 531.3 eV correspond to the lattice oxygen in the from oxide and hydroxide form of Ir. From the reported literature, peak at B.E. of 531.3 eV could be responsible for the presence of Ir-O or Ir-OH bond in the catalyst. Also, peak at B.E. = 531.3 eV was attributed to various oxygen defects present in the catalyst, which arise from O^{2-} , O^- or surface adsorbed oxygen species.⁴⁴ Presence of larger peak at BE = 533.01 eV could be assigned to adventitious carbon species which originate from diminutive fraction of oxygen components present in carbon.^{42,43} These observations suggest that oxygen defect sites in this catalyst system may help to produce H_2 and oxygen via splitting of H_2O involved in the mechanistic pathway during furfural hydrogenation to 2-MF. This is analogues with water gas shift reaction and oxygen evolution reactions by using Ir catalysts systems.⁴⁵

Figure S1 depicts the C1s core level spectra of monometallic fresh 5% Ir/C with corrected C1s at B.E. 284.6 eV. After deconvolution, four different peaks appeared with B.E. at 284.16 eV, 284.59 eV, 284.78 eV and 286.33 eV. Out of these, peaks at BE = 284.13 eV, 284.59 eV and 284.78 eV corresponded to the presence of adventitious carbon and C-C bond, respectively. While, the peak at BE = 286.33 eV represents the existence of C-OH or C-O-C bonds.⁴⁶ However, there is no detectable C=O and O-C=O species at BE of 287.9 eV and 288.8 eV on the catalyst surface. Contribution of the above peaks suggests the even deposition of iridium particles over carbon supports which existed in metallic as well as its different oxide states.

TEM

The particle size and morphological features of fresh and spent Ir/C catalysts were determined by TEM as shown in Figures 3A and 3B.

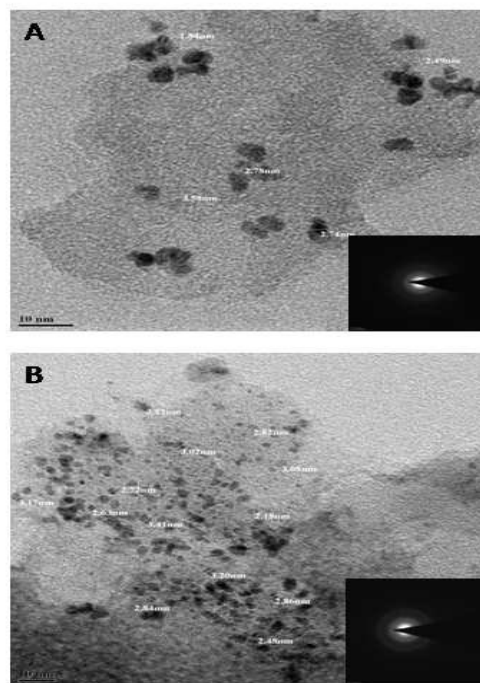


Figure 3: TEM analysis of 5% Iridium/Carbon with SAED pattern (inset figures A) Fresh Ir/C B) Used Ir/C)

Supported Ir particles on carbon showed uniform distribution having spherical morphology and particle size in the range of 2.4 to 3.6 nm.⁴⁷ SAED pattern shown as inset of Fig 3A with distinct diffuse rings was in close agreement with XRD results. Average interlayer spacing calculated as 0.2112 nm was for the characteristic phase of graphitic carbon or iridium monolayer formed on the carbon surface. Similar findings were observed for spent 5% Ir/C catalyst sample. Interestingly, particle size in the used catalyst was slightly reduced in the range of 2.1 to 3.3 nm.⁴⁷ Indeed, increase in intensity of three diffuse rings in SAED pattern implied the formation of crystalline phases over

the support. The crystallinity observed may be due to intercalation of iridium with the carbon support with d spacing of around 0.2095 nm.^{48,49}

Ammonia TPD

Since hydrodeoxygenation of furfural to give 2-MF is favoured by acid catalysis²⁵, total acid strength of 5% Ir/C catalyst was determined by NH₃-TPD and the results are shown in Figure S2 and Table S2. Fresh catalyst showed three distinct peaks in all three regions. Typical broad desorption peak in the temperature range of 40–200 °C with maxima centred at 64 °C indicated the presence of weak acid sites. The desorption peak present in the range of 200–400 °C centred at 347 °C implied the presence of medium acidic sites while, strong intense peak observed above 400 °C centred at 714 °C implied the presence of very strong acidic sites. Total acidity in terms of ammonia desorbed per unit weight of catalyst for the fresh catalyst was 0.1633 mmol g⁻¹ while for the spent catalyst, it was slightly higher as 0.1669 mmol g⁻¹. The reason for such significant acid strength was due to the presence of oxide species of iridium the presence of which was confirmed by XRD and XPS as discussed above. Brønsted acidity was confirmed by Py-IR technique where, distinct absorption band at 1541 cm⁻¹ clearly confirmed the presence of Brønsted acidity, as shown in Figure S3.

Activity testing

Among several products possible from FFR, formation of 2-MF is via selective removal of oxygen from formyl group through selective hydrodeoxygenation suppressing the competitive ring hydrogenation as well as ring opening products. For achieving this, initially catalysts with iridium on different supports like C, Al₂O₃, MMT, and ZrO₂ were screened for furfural hydrogenation and the results are given in Figure 4.

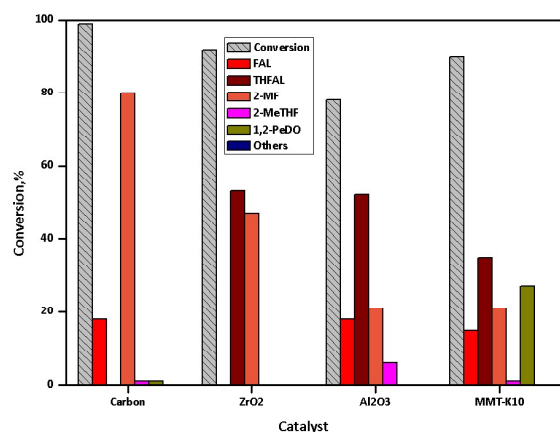


Figure 4: Metal on different support. **Reaction conditions:** furfural, 2.5g; solvent (IPA), 95ml; catalyst (4% Ir), 0.25g, temp., 220°C; H₂ pressure, 100 psig; Agitation speed, 1000 rpm, time, 5h.

It was observed that 4% Ir on different supports showed near about similar furfural conversion while, the selectivity to 2-MF was in the following order, C>ZrO₂>Al₂O₃=MMT. ZrO₂

supported Ir catalyst gave selectivity of 46% to 2-MF and 52% to THFAL. Both Al₂O₃ and MMT-K10 supported catalysts preferentially formed FAL (35%) along with 2-MF up to only 21% with THFAL still remaining higher at 52%. However, incorporation of Ir on MMT-K10, resulted in significant (27%) formation of open chain product like 1,2-PeDO which could be ascribed to the presence of parent surface acidity of MMT K10.⁵⁰ Among all the catalysts screened very interestingly, 4% Ir/C catalyst was found to be the best catalyst for selective production (80%) of 2-MF via furfural hydrogenation in a single step. In order to further maximize 2-MF selectivity, initially metal loading effect was studied in the range of 1% to 6%.

Table 1: Effect of metal loading

Sr	Metal load, %	Conv. %	Selectivity, %						
			II	IV	V	VI	VII + VIII	TON	TOF h ⁻¹
1	1	90	48	-	52	-	-	280	560
2	2	94	28	-	70	-	2	208	416
3	4	99	18	-	80	-	2	128	256
4	5	99	-	1	95	4	-	158	316
5	6	99	-	5	87	8	-	130	264

Reaction conditions: furfural, 2.5g; solvent (IPA), 95ml; loading, 0.25g, temperature, 220°C; H₂ pressure, 100 psig; Agitation speed, 1000, time, 5h.

Table 1 shows that increasing Ir loading from 1 to 4% favoured increase in 2-MF selectivity from 52% to 80% at the cost FAL selectivity which depleted from 48% to 18% (entries 1-3). Subsequent increase in metal loading up to 5% resulted in complete consumption of FAL with concomitant formation of 2-MF to the extent of about 95% (Table 1, entry 4). Further, increase in Ir loading up to 6% influenced the selectivity of 2-MF to drop down to 87% with increase in next step ring hydrogenated products (Table 1, entry 5). Thus, appropriate Ir metal loading favoured selective formation of 2-MF, above which further hydrogenation of 2-MF takes place due to availability of higher amount of active sites. Respective catalytic activity calculated in terms of TON and TOF at low conversion levels are given in Tables 1 and S3. A typical conversion and selectivity Vs time profile of FFR hydrogenation over 4% Ir/C is shown in Figure 5. Both conversion and 2-MF selectivity linearly increased with progress in reaction time. At the end of first hour, 71% FFR conversion was achieved which steadily reached to 99% until the reaction reached to 5th h. Initially in the first hour, 56% selectivity to FAL was observed which then decreased linearly to 4% during 4th hour and finally diminished after 5th hour of the reaction. Similarly, 2-MF selectivity of 43% observed during 1st hour of reaction time steadily enhanced to 95% at the end of 5th hour. On the other hand, formation of 2-MeTHF and THFAL was very negligible and remained almost constant throughout the reaction. These results certainly indicate that 5% Ir/C was highly selective to 2-MF formation which proceeded through FAL intermediate. In order to confirm the later, hydrogenation of the intermediate

ARTICLE

Journal Name

FAL was carried out under standard optimized reaction conditions which gave maximum selectivity to 2-MF and small amount of THFAL (5%) and 2-MeTHF (10%) (Table S4). Similarly, starting with 2-MF as a substrate, complete selectivity to 2-MeTHF was achieved. From these results, a plausible reaction pathway is shown in Scheme 2. Above transformations may be due to structural role of different iridium phases which are exposed during the hydrogenation, as discussed later.

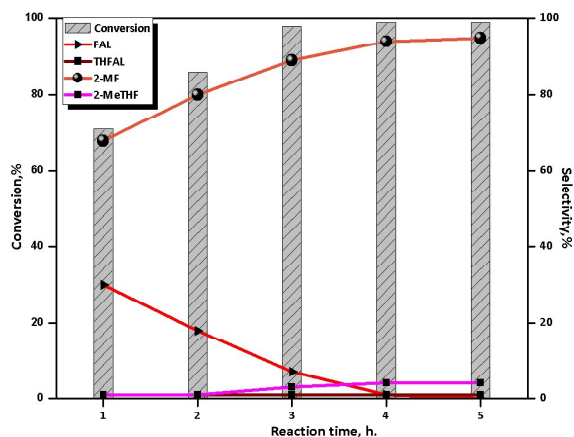
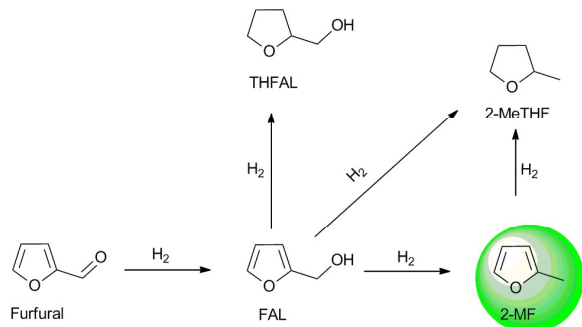


Figure 5: Conversion and selectivity vs time profiles **Reaction conditions:** furfural, 2.5g; solvent (IPA), 95ml; catalyst, 0.25g, temp., 220°C; H₂ pressure, 100 psig; Agitation speed, 1000 rpm, time, 5h.



Scheme 2: Plausible reaction pathway

As 5% Ir/C catalyst showed maximum selectivity to 2-MF further reaction parameter optimization studies for furfural hydrogenation were carried out over 5% Ir/C catalyst.

Effect of temperature

Effect of temperature on conversion of furfural and product distribution was studied in a range from 140–240 °C. Figure 6 shows that at a lower temperature of 140 °C, the conversion of furfural was 70 % with 68 % selectivity to first step hydrogenation product, FAL while selectivity to 2-MF obtained was 25%. With increase in reaction temperature from 140 to 220 °C, a trend of linear increase 2-MF selectivity from 25% to

95% with complete conversion of furfural was observed. This increase in 2-MF selectivity with increase in temperature was accompanied by decrease in FAL selectivity from 68% to nil. With further increase in reaction temperature up to 240 °C, marginal decrease in selectivity to 2-MF from 95% to 87% was observed. A small amount of THFAL (~ 5%) was observed even at lowest temperature of 140 °C which slightly increased up to 200 °C and became almost nil at 220 °C. However, 2-MeTHF formation was observed only at 180 °C which increased linearly to ~ 10 % up to 240 °C. Thus ring hydrogenation of 2-MF to some extent was facilitated only at higher temperature over Ir/C catalyst.

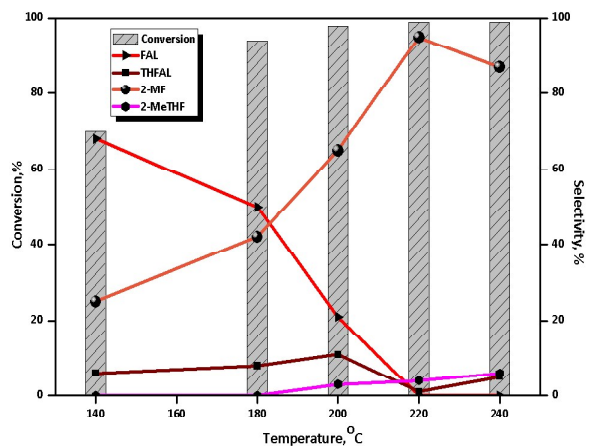


Figure 6: Effect of temperature on conversion and selectivity of furfural hydrogenation. **Reaction conditions:** furfural, 2.5g; solvent (IPA), 95ml; catalyst, 0.25g; H₂ pressure, 100 psig; Agitation speed, 1000 rpm, time, 5h.

Effect of H₂ pressure

Figure 7 shows influence of H₂ pressure in the range 100–750 psig on product distribution of furfural hydrogenation by keeping all other parameters constant.

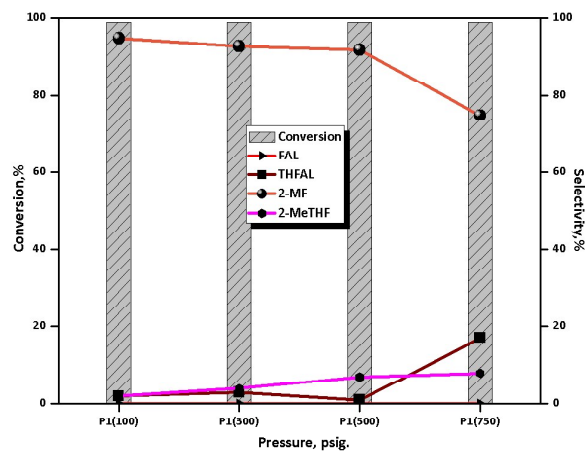


Figure 7: Effect of H₂ pressure on conversion and selectivity of furfural hydrogenation **Reaction conditions:** furfural, 2.5g; solvent (IPA), 95ml; catalyst, 0.25g, temp., 220 °C; Agitation speed, 1000 rpm, time, 5h.

Complete conversion of FFR was achieved even at lowest H₂ pressure of 100 psig. While, 2-MF selectivity remained

constant at ~95% up to 500 psig but dramatically dropped down to 75% at enhanced pressure of 750 psig with a subsequent increase in THFAL (17%) selectivity. This was due to ring hydrogenation at higher H₂ pressure to give 2-MeTHF. Thus, increase in pressure to 500 psig, 2-MF selectivity was 92% with 7% selectivity to 2-MeTHF. With further increase in pressure to 750 psig, 2-MF selectivity dropped down to 75% with higher selectivity to THFAL (17%) and 2-MeTHF (8%). Hence, the low H₂ pressure of 100 psig would be more favourable for furfural hydrodeoxygenation process to give 2-MF.

Effect of catalyst loading

Catalyst loading effect in the range of 0.12g to 0.4g was studied at 100 psig H₂ keeping all other reaction conditions constant.

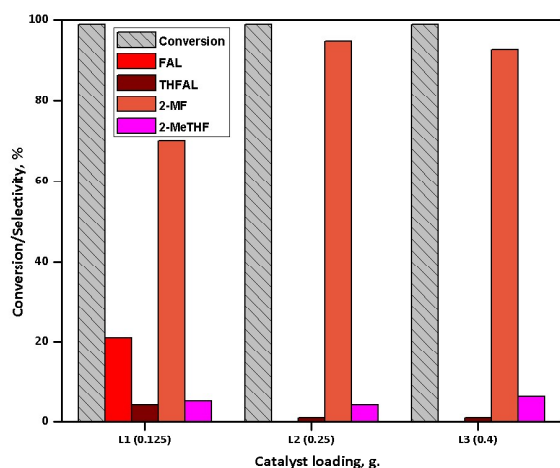


Figure 8: Effect of catalyst loading on conversion and selectivity of furfural hydrogenation. **Reaction conditions:** furfural, 2.5g; solvent (IPA), 95ml; catalyst, 0.25g, temp., 220 °C; H₂ pressure, 100 psig; Agitation speed, 1000 rpm, time, 5h.

Figure 8 shows that for all catalyst loadings, complete conversion was achieved. At lower catalyst loading of 0.12g, 2-MF selectivity was as low as 70% as FAL formation was 21% indicating the insufficient active sites available for deoxygenation via FAL. As the catalyst loading increased to 0.25g, 2-MF selectivity reached to 95% with decrease in FAL selectivity from 21% to nil. This trend remained the same with further increase in catalyst loading to 0.4g. However, minor ring hydrogenation of 2-MF resulted in 6% selectivity to 2-MeTHF.

Study of effect of substrate loading showed that increasing the substrate loading from 2.5g to 7.5g, selectivity to 2-MeF decreased from 95% to 66% as well as FFR conversion decreased to 78% with increase in FAL selectivity to 31% shown in Figure S4.

Above results imply that 5% Ir/C catalyst selectively prefers only side chain hydrogenation rather than ring hydrogenation or ring opening products and giving very high selectivity to 2-MF through hydrodeoxygenation of furfural. Catalyst stability and recyclability of 5% Ir/C catalyst at 100 psig was also tested by subsequent reuse runs as shown in Figure 9.

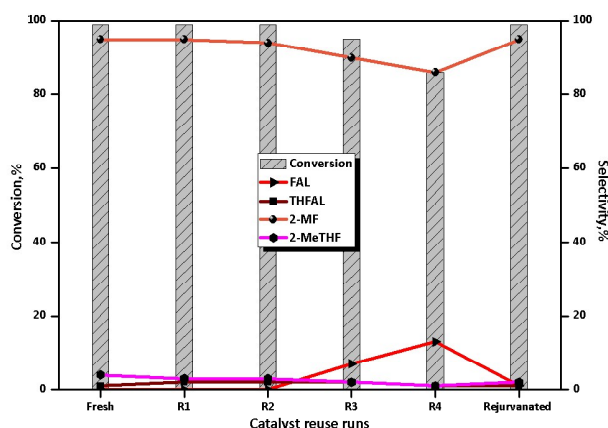


Figure 9: Catalyst recycle study. **Reaction conditions:** furfural, 2.5g; solvent (IPA), 95ml; catalyst, 0.25g, temp., 220 °C; H₂ pressure, 100 psig; Agitation speed, 1000 rpm, time, 5h.

Initially at optimized H₂ pressure 100 psig (Figure 9), after completion of the reaction, reaction crude was separated by decantation after settling the catalyst and fresh charge was fed to the reactor and the reaction was continued. Catalyst was active till 4th use. Till 3rd reuse selectivity pattern was the same as for fresh catalyst however, after 4th reuse 2-MF selectivity dropped down from 95% to 86% along with increase in FAL selectivity from nil to 13 % with a negligible decrease in 2-MeTHF from 4% to 2%. This was also associated with decrease in conversion from 99% to 87 %. Decrease in conversion and selectivity may be due to catalyst poisoning causing unavailability of active metallic iridium sites. More importantly, activity of the reused 5%Ir/C catalyst could be regained by activating the spent catalyst in H₂ environment and the catalyst showed complete FFR conversion with similar 2-MF selectivity for next reuse. In order to compare stability of the catalyst, catalyst recycle runs were also carried out at high pressure (500 psig) and results are shown in Figure S5. Surprisingly, 2-MeTHF selectivity increased during successive recycles with decrease in 2-MF selectivity. In order to check the possibility of iridium leaching, hot filtration test was performed as shown in Figure 10. After 1st h, the reaction was stopped and the catalyst was removed by filtration. The reaction was continued with the filtrate devoid of catalyst. As no any change in conversion of furfural was observed, it could be inferred that the catalyst was quite stable and non-leachable under the standard optimized reaction conditions. Results were crossed checked by ICP-OES experiments. At the same time, solvent reuse study were also done where almost no change in conversion as well as in 2-MF selectivity were observed. (Table S5)

XRD of used 5% Ir/C catalyst (Figure S6) showed the signals at same peak positions without any significant changes. From TEM analysis, morphology also was found to be the same (spherical) with particle size of 1.5 to 3 nm as that of the fresh sample, which is discussed earlier (Figure 3B).

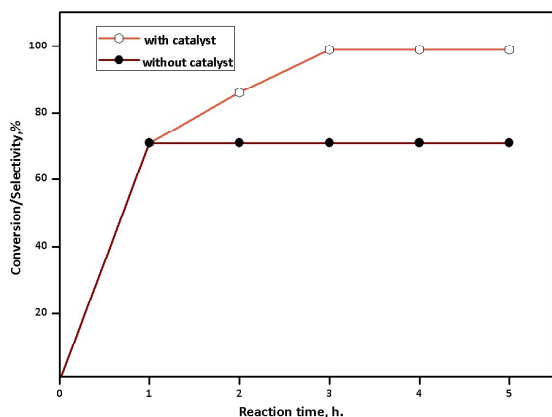


Figure 10: Catalyst leaching test. **Reaction conditions:** furfural, 2.5g; solvent (IPA), 95ml; catalyst, 0.25g, temp., 220 °C; H₂ pressure, 100 psig; Agitation speed, 1000 rpm, time, 5h.

In order to establish and check effect of successive catalyst recycles on catalyst surface, XPS analysis of spent catalysts were done shown in Figure 11.

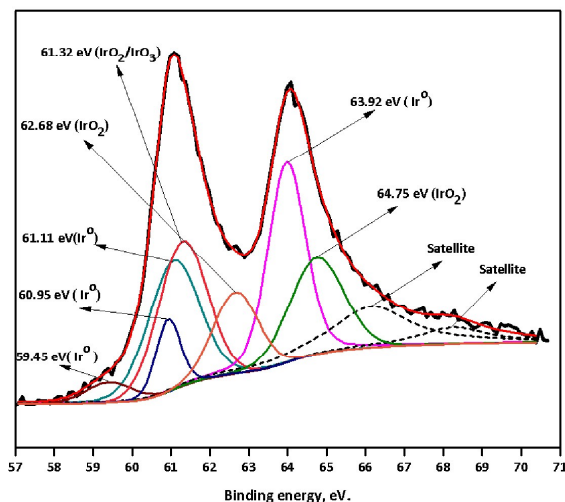


Figure 11: XPS spectrum of 5% Ir/C used catalyst

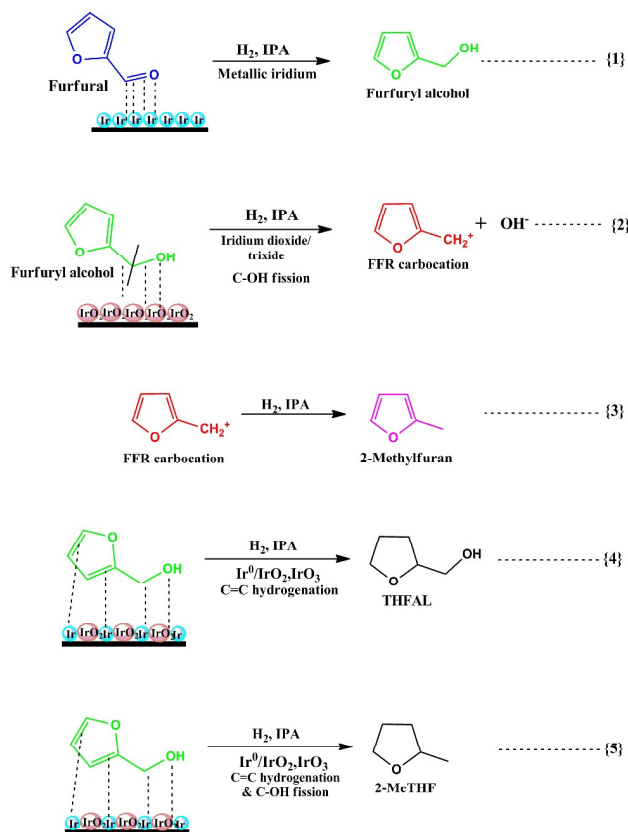
It was found that iridium was present as Ir⁰, IrO₂ and IrO₃. The peaks at B.E. of 60.95 eV and 63.93 eV corresponded to metallic iridium while, those at B.E. of 61.11 eV, 61.32 eV, 62.68 eV and 64.75 eV represented various oxides of iridium, such as IrO₂ or IrO₃ as 4f_{7/2} and 4f_{5/2}, respectively. However, two satellite peaks observed at B.E. of 66.11 eV and 68.18 eV could be ascribed to uneven shaking of protons.^{39,40,51} After careful comparison of XPS of fresh and used 5% Ir/C catalyst, it was observed that total percentage of metallic Ir decreased and that of oxide increased in the used sample. It may be because of interaction of metallic Ir with OH⁻ species removed from furfuryl alcohol via hydrodeoxygenation, in spite of presence of hydrogen. This clearly suggests that Ir has a strong affinity towards oxygen.

Moreover, after deconvolution of O1s and C1s of used 5% Ir/C catalyst (Figures S7 & S8), the main peaks centred at B.E. of 532.8 eV consisted of six peaks as compared to fresh Ir/C catalyst having B.E. of 531.8 eV. Among six peaks, the peak at B.E. of 529.6 eV corresponded to lattice oxygen, while another set of peaks at B.E. of 531.5 eV and 531.96 eV represented the features of hydroxyl and ether groups, which may arise from oxygen defects. Similarly, there were two peaks at B.E. of 533.06 eV and 533.86 eV that implies adsorbed C=O groups, while peak at BE of 534.52 eV could be assigned to the presence of C=O group originating from adsorption through π as well as α - β unsaturated bond linkages of furfural and furfuryl alcohol during successive recycle runs over the catalyst surface. This is in good agreement with the results obtained by deconvolution C1s spectrum of used Ir/C (Figure S7) catalyst. The five different peaks with binding energies of 284.45 eV, 284.48 eV, 285.22 eV, 286.47 eV and 288.34 eV corresponded to surface composition of C-C bond and adventitious carbon. Another set of peaks at BE of 286.46 eV and 288.31 eV were associated with the presence of C-OH and C=O species. Upward shift of peaks implies the strong association of metal, substrate and products with carbon support.^{44,46} Total composition of species is calculated by corresponded area of iridium, oxygen and carbon along with their respective functional groups (Table S6) where increase in oxygen content on catalysts surface clearly indicated that there was depletion in metallic iridium content with respect to increase oxide form of Ir, which is in line during successive recycle runs at standard optimized conditions.

Plausible reaction mechanism

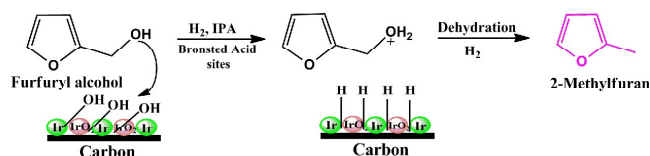
Our catalyst possesses coexistence of all three phases of iridium viz. Ir⁰, IrO₂, and IrO₃. As shown in Scheme 3, initially, furfural gets adsorbed on the surface through π -bond of formyl group forming furfuryl alcohol selectively, under hydrogenation conditions. Later interaction of FAL with IrO₂ through C-OH in contrast to least absorption affinity of C=C bond for IrO₂, leads to the formation 2-MF in a single step. As stated, iridium is well known for oxygen evolution reaction in which water molecule splits into the H⁺ and OH⁻.^{40,51-53} We hypothesized that iridium dioxide induces the splitting of FAL into [C₅H₅O⁺] and [OH⁻] and then in situ reaction of [OH⁻] with external H₂ resulted in the formation of water molecule and free hydride i.e. [H⁻]. Later in association with [C₅H₅O⁺] species with free hydride, resulted in the formation of 2-MF. It is also reported that defects present in oxygen as well as availability of Ir³⁺ and Ir⁴⁺ sites are helpful to alter the mechanistic way rather hydrogenation and favors hydrodeoxygenation of furfural to give 2-MF.⁴⁰ Above hypothesis was validated with some control experiments and XPS studies of fresh and used 5% Ir/C catalyst samples (Figures S7, S8, S10 and Table S3, S5). Use of 5% Ir/C before NaBH₄ reduction showed somewhat lower furfural conversion but high selectively to 2-MF (Figure S9). Moreover, part of FAL molecules which were strongly adsorbed on the surface through C=C bond led to the formation of THFAL and 2-MeTHF which were also by-products

of the reaction, formed at higher catalyst loading and high temperature. Simultaneous absorption of FAL switches the product selectivity to either 2-MeTHF or THFAL.^{54,55} Mass spectrum of 2-MF is given in Figure S11.



Scheme 3: Plausible reaction mechanism over 5% Ir/C

As 5% Ir/C possesses Brönsted acidity, selective formation of 2-MF from furfural can be explained by alternate pathway also. Initially, furfural gets converted to FAL through hydrogenation of C=O bond over metallic iridium sites. Subsequently, FAL gets protonated to forms the unstable carbocation whose subsequent dehydration followed by hydrogenation in presence of H₂ gives 2-MF selectively, as shown in Scheme 4.



Scheme 4: Acid catalysed plausible reaction mechanism over 5% Ir/C

Conclusions

Carbon supported Ir catalysts with varying Ir loadings of 1 to 6% were prepared and screened for furfural hydrogenation to 2-MF. HR-TEM revealed that the particle size of iridium

particles in the range of 2 to 3 nm with an excellent dispersion on carbon support, confirmed by respective SAED pattern which remained almost same even after catalyst reuse. Different phases of iridium were confirmed by XPS analysis and respective acidity was calculated by NH₃-TPD. Systematic study with varying Ir loading results in different individual 2-MF selectivities. Under optimized reaction conditions, 5% Ir/C catalyst gave 95% 2-MF selectivity at low H₂ pressure i.e. 100 psig suppressing other by product formation. Varying different reaction parameters like temperature, pressure, catalyst loading etc. product selectivity could be tuned to ring hydrogenation products. At lower catalyst loading 1%, both FAL and 2-MF were formed with almost equal selectivities. Similarly, at low temperature 140 °C, conversion dropped down to 70% with 68% selectivity to FAL while, highest temperature of 240 °C favored ring hydrogenation product i.e. 2-MeTHF (87%). With the help of some control experiments, in proposed reaction mechanism, crucial role of IrO₂ species is shown which facilitates the selective formation of 2-MF from FAL. Similar way, acid mediated mechanism FR to 2-MF mechanism is also given. The presence of relevant species responsible for these transformations were characterized by XPS analysis. Interestingly, catalyst was found to be very stable at low pressure (100 psig) even after four recycles and showed similar activity after its rejuvenation by hydrogen. No leaching of iridium metal was observed as confirmed by hot filtration test and by ICP-OES analysis.

Conflicts of interest

The manuscript was written through contributions of all authors. All authors have given approval to the final version of the manuscript. "There are no conflicts to declare".

Acknowledgements

One of the authors NSD gratefully acknowledges Department of Science and Technology (DST) New Delhi, for financial support to him.

Abbreviations:

FFR: furfural; FAL: Furfuryl alcohol; THF: Tetrahydrofuran; 2-MF: 2-methyl furan; THFAL: Tetrahydrofurfuryl alcohol; CPO: Cyclopentanone; 2-MeTHF: 2-Methyltetrahydrofuran; PeDO: Pentanediols

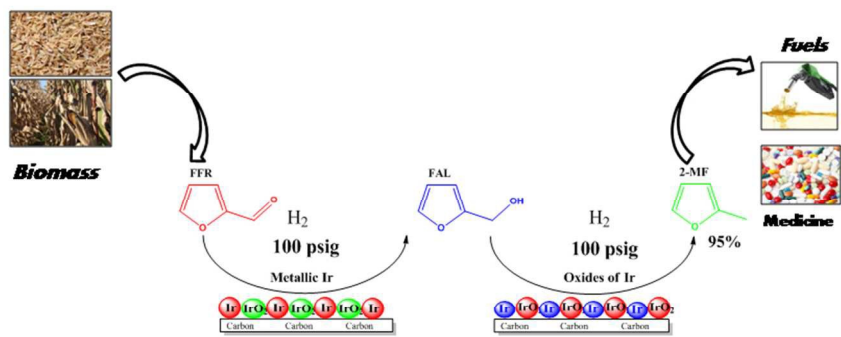
References

- 1 J. C. S. Ruiz and J. A. Dumesic, *Energy Environ. Sci.*, 2011, **4**, 83-99.
- 2 D.M. Alonso, J.Q. Bond and J.A. Dumesic, *Green Chem.* 2010, **12**, 1493–1513.

ARTICLE

Journal Name

- 3 J. A. Corma, S. Iborra and A. Velty, *Chem. Rev.*, 2007, **107**, 2411–2502.
- 4 R. D. Cortright, R.R. Davda and J.A. Dumesic, *Nature.*, 2002, **418**, 964–967.
- 5 A. Martinez-Garcia, M. Ortiz, R. Martinez, P. Ortiz and E. Reguera, *Ind. Crop Prod.*, 2004, **19**, 99–106.
- 6 Rodiansono, S. Khairi, T. Hara, N. Ichikuni and S Shimazu, *Catal. Sci. Technol.*, 2012, **2**, 2139–2145.
- 7 R. Mariscal, P. M. Torres, M. Ojeda, I. Sádaba, and M. L. Granados., *Energy Environ. Sci.*, 2016, **9**, 1144–1189.
- 8 H. Ren, W. Yu, M. Saliccioli, Y. Chen, Y. Huang, K. Xiong, D.G. Vlachos and J.G. Chen, *ChemSusChem*, 2013, **6**, 798–801.
- 9 P. Panagiotopoulou, N. Martin, D. G. Vlachos, *Journal of Mol. Cat. A: Chemical*, 2014, **392**, 223–228.
- 10 L. Hu, G. Zhao, W. Hao, X. Tang, Y. Sun, L. Lin, S. Liu, *RSC Adv.*, 2012, **2**, 11184–11206.
- 11 C.-C. Chang, S.K. Green, C.L. Williams, P.J. Dauenhauer, W. Fan, *Green Chem.* 2014, **16**, 585–588.
- 12 D. Wang, C.M. Osmundsen, E. Taarning, J.A. Dumesic, *ChemCatChem*, 2013, **5**, 2044–2050.
- 13 S. Wei, H. Cui, J. Wang, S. Zhuo, W. Yi, L. Wang and Z. Li, *Particuology*, 2011, **9**, 69–74. **13**
- 14 C. Wang, H. Xu, R. Daniel, S. Shuai and X. Ma, *Fuel*, 2013, **103**, 200–.
- 15 X. Ma, C. Jiang, H. Xu, H. Ding and S. Shuai, *Fuel*. 2014, **116**, 281–291
- 16 J. P. Lange, E.V.D. Heide, J.V. Buijtenen and R. Price, *ChemSusChem.*, 2012, **5**, 150–166.
- 17 K. Xiong, W. Wan and J. G. Chen, *Surface Science*, 2016, **652**, 91–97.
- 18 W. Yu, K. Xiong, N. Ji, M.D. Porosoff and J.G. Chen, *J. Catal.*, 2014, **317**, 253–262.
- 19 A. S. Sitthisa, T. Sooknoi, Y.G. Ma, P.B. Balbuena and D.E. Resasco, *J. Catal.*, 2011, **277**(1), 1–13.
- 20 S. Sitthisa and D. Resasco, *Catal. Lett.*, 2011, **141**, 784–791
- 21 S. Sitthisa, W. An and D.E. Resasco, *J. Catal.*, 2011, **284**, 90–101.
- 22 K. Yan and A. Chen, *Fuel*, 2014, **115**, 101–108.
- 23 K. Yan and A. Chen, *Energy*, 2013, **58**, 357–363.
- 24 P. Panagiotopoulou, N. Martin and D.G. Vlachos *J. of Mol. Cat. A: Chem.* 2014, **392**, 223–228.
- 25 P. Panagiotopoulou and D.G. Vlachos, *Appl. Catal. A: Gen.* 2014, **480**, 17–24.
- 26 G. S. Hutchings, W. Luc, Q. Lu, Y. Zhou, D. G. Vlachos and F. Jiao, *Ind. Eng. Chem. Res.*, 2017, **56**, 3866–3872.
- 27 D. Scholz, C. Aellig, and I. Hermans, *ChemSusChem*, 2014, **7**(1), 268–275.
- 28 L. Wang, F. S. Xiao, *Green Chem.* 2014, **17**, 24–39.
- 29 J. Lee, Y. T. Kim, and G. W. Hube, *Green Chem.*, 2014, **16**, 708–718.
- 30 X. Chen, H. Li, H. Luo and M. Qiao, *Appl. Catal. A.*, 2002, **233**, 13–20.
- 31 John G. M. Bremner, Richard K. F. Keeys, *J. Chem. Soc.* **1947**, 1068–1080.
- 32 K. Xiong, W.-S. Lee, A. Bhan and J.G. Chen, *ChemSusChem*, 2014, **7**(8), 2146–2149.
- 33 W.S. Lee, Z. Wang, W. Zheng, D.G. Vlachos and A. Bhan, *Catal. Sci. Technol.*, 2014, **4**, 2340–2352.
- 34 A. Banerjee and S. H. Mushri, *ChemCatChem*, 2017, **9**, 2828–2838.
- 35 N.S. Date, N.S. Biradar, R.C. Chikate and C.V. Rode, *Chemistry Select*, 2017, **2**, 24–32.
- 36 B. J. Borah, S. J. Borah, K. Saikia and D. K. Dutta, *Appl. Catal. A: Gen.*, 2014, **469**, 350–356.
- 37 P. Devarly, Y. Kartika, N. Indraswati and S. Ismadji, *Chem. Eng. J.*, 2008, **140**, 32–42.
- 38 A) R. Mane, S. Patil, M. Shirai, S. Rayalu, C. Rode, *Applied Catalysis B: Environmental*, 2017, **204**, 134–146. B) A. Irshad, N. Munichandraiah, *ACS Appl. Mater. Interfaces*, 2015, **7** (29), 15765–15776
- 39 G.K. Wertheim and H. J. Guggenheim, *Phys. Rev. B: Condens. Matter Mater. Phys.* 1980, **22**, 4680–4683.
- 40 S. J. Freakley, J. Ruiz-Esquius and D. J. Morgan *Surf. Interface Anal.*, 2017, **49**, 794–799.
- 41 A) V. Pfeifer, T. E. Jones, J. V. Vélez, C. Massué, M. T. Greiner, R. Arrigo and M. Hashagen, *Phys. Chem. Chem. Phys.*, 2016, **18**, 2292–2296. B) S. J. Freakley, J. Ruiz-Esquius and D. J. Morgan *Surf. Interface Anal.*, 2017, **49**, 794–799
- 42 V. Pfeifer, T. E. Jones, J. J. Velasco Vélez, C. Massué, R. Arrigo, D. Teschner and M. Hashagen. *Surf. Interface Anal.*, 2016, **48**, 261–273.
- 43 R. Kötz, H. Neff and S. J. Stucki, *Electrochem. Soc.* 1984, **131**, 72–77.
- 44 R. D. Smith, B. Sporinova, R. D. Fagan, S. Trudel and C. P. Berlinguette. *Chem. Mater.* **2014**, **26**, 1654–1659.
- 45 X. Zhang, J. Qin, Y. Xue, P. Yu, B. Zhang, L. Wang and R. Liu, *Sci. Rep.*, 2014, **4**, 4596–4605.
- 46 A. Jha, D.W. Jeong, J. O. Shim, W. J. Jang, Y. L. Lee, C. V. Rode, and H. S. Roh, *Catal. Sci. Technol.*, 2015, **5**, 2752–2760.
- 47 J. F. Moulder, W. F. Stickley, P. E. Sobol and K. D. Bomben, *Handbook of X-ray Photoelectron Spectroscopy*, PerkinElmer, Waltham, Massachusetts, USA, **1992**.
- 48 T. Nakagawa, N. S. Bjorge and R.W. Murray, *J. Am. Chem. Soc.*, 2009, **131**, 15578–15579.
- 49 Y. Zhao, E. A. Hernandez-Pagan, N. M. Vargas-Barbosa, J. L. Dysart and T. E. Mallouk, *J. Phys. Chem. Lett.*, 2011, **2**, 402–406.
- 50 N. S. Date, R.C. Chikate, H.S. Roh and C.V. Rode. Date, N.S., *CatalysisToday*, (2017), <http://dx.doi.org/10.1016/j.cattod.2017.08.002>
- 51 A. Minguzzi, C. Locatelli, O. Lugaresi, E. Achilli, G. Cappelletti, M. Scavini, M. Coduri, P. Masala, B. Sacchi, A. Vertova, P. Ghigna and S. Rondinini, *ACS Catal.*, 2015, **5**, 5104–5115.
- 52 D. F. Abbott, D. Lebedev, K. Waltar, M. Povia, M. Nachtegaal, E. Fabbri, C. Copéret and T. J. Schmidt. *Chem. Mater.*, 2016, **28**, 6591–6604.
- 53 B. Seemala, C.M. Cai, C.E. Wyman and P. Christopher, *ACS Catal.*, 2017, **7**, 4070–4082.
- 54 Daming Shi and John M. Vohs, *ACS Catal.*, 2015, **5**, 2177–2183.
- 55 Y. Nakagawa, M. Tamura and K. Tomishige, *ACS Catal.*, 2013, **3**, 2655–2668.



254x190mm (96 x 96 DPI)